Local Tomography Study of the Fracture of an ERG Metal Foam

Tao Zhang, Eric Maire, Jérôme Adrien, Patrick Onck, Luc Salvo

Local Tomography Study of the Fracture of an ERG Metal Foam**

By Tao Zhang,* Eric Maire, Jérôme Adrien, Patrick R. Onck and Luc Salvo

As one of the most important analysis techniques for non-destructive imaging, X-ray tomography has been widely used in materials science, medical science, and industry to evaluate the behavior of porous materials. By using this method, a three dimensional volume can be inspected in order to visualize in situ the progress of damage in materials and this can be analyzed qualitatively and quantitatively. In the present study, we have used X-ray tomography to investigate the fracture behavior of an ERG open cell aluminum foam. The process of damage development of a sample undergoing tension and the relation between the inter-metallics and the cracks can be observed totally by the X-ray tomography set-up. Local tomography has in particular been used to image the microstructure at high resolution. A finite element model has also been developed in order to simulate this process of the damage using the 3D data obtained by the tomography.

Cellular solids, such as polymer and glass foams (or wools), have long been used for thermal insulation to exploit their low thermal conductivity. Ceramic foams have been used for instance as filters and catalyst supports. A major use of cellular solids is in packaging, since they exhibit good energy absorption properties. In the last three decades, metallic foams, the newest class of cellular solids have emerged with an interesting set of properties, see ref.[1] for a review of these properties.

X-ray computed tomography (XRCT) has appeared recently to be a very powerful tool allowing to characterize the microstructure of cellular materials. It clearly appears now to be one of the most versatile techniques capable to provide non-destructive three-dimensional (3D) images of a complete sample of cellular material.[2–7]

In most of these studies, the Laboratory-based version of XRCT (LXRCT, as opposed to the synchrotron based version SXRCT) has been used. A large number of laboratory-based tomographs are now available in different academic institutions and industrial laboratories and they are widely accessible. The resolution available using LXRCT is more than sufficient to visualize the cellular microstructure of cellular materials. Typical resolutions from a few microns up to 50 μm are then commonly used. These images are also often obtained during in situ mechanical tests (tension or compression including indentation). This has proved to be a very efficient technique to analyze the effect of the architecture of the material on the fracture process in tension[8,9] or the collapse process in compression.[10] These images can also be quite straightforwardly used to produce finite element (FE) models of the actual architecture of the foams. This has been shown for example in ref.[9] and used many times in the literature since then.[11–13]

Under these conditions of medium resolution, the actual microstructure of the solid metal (i.e. that of the struts and cell walls) cannot be resolved. It has been shown however in ref.[14–17] that inter-metallics present in metal foams play a key role at the local scale on the fracture process. This has been observed on ERG aluminum-based metal open cell foams in several of these studies (see e.g.[16,17]).

In this paper, we will use LXCRT images of ERG foam at two different scales during an in situ tensile test to analyze the global fracture process but also the effect of the microstructure of the metal inside the struts on the local

[*] *T. Zhang, Dr. E. Maire, Dr. J. Adrien*
MATEIS UMR 5510, Université de Lyon St-Exupery Building, 3rd Floor, 25 Avenue Jean Capelle, 69621 Villeurbanne, France
E-mail: eric.maire@insa-lyon.fr
Prof. P. R. Onck
Zernike Institute for Advanced Materials, University of Groningen, Nijenborgh 4, NL-9747 AG Groningen, The Netherlands
Dr. L. Salvo
SIMAP-GPM2, Université de Grenoble – CNRS, Domaine Universitaire BP 46 38402 Saint Martin d'Heres, France
E-mail: luc.salvo@simap.grenoble-inp.fr

[**] *The authors would like to thank the Région Rhônes Alpes in France for funding the PhD work of T. Zhang. The collaboration was favoured by HETMAT, a European Research Group funded by the French CNRS.*

fracture process. The high resolution will be acquired in the so called ''local'' tomography mode, where the sample is larger than the field of view of the detector. The low resolution image in the initial state will be used to produce a FE model of the structure of the foam and the FE calculation will be used to analyze the fracture process experimentally observed during the in situ tensile test.

In Situ XRCT

A parallelepiped shaped 15 mm × 10 mm × 4 mm sample of ERG foam was cut. One standard M5 screw was glued with epoxy at each end of the sample to allow an easy attachment to the two grips of the tensile stage. During the gluing process, we took care of maintaining the alignment of the two screws using a little device especially designed for this purpose. The tensile rig is shown in an unmounted state in Figure 1. The bottom part was first mounted on the rotating stage of the tomograph. Then the sample was screwed in the top grip, attached through the force sensor to an aluminum tube, surrounding the entire sample and acting as the structural part of the rig (i.e. replacing the two classical structural beams of a standard tensile rig). This aluminum tube is 1 mm thin and its external diameter is about 16 mm. It is rather transparent to the X-rays and absorbs in the same manner in each angular position. It is then not perturbing the reconstruction of the tomograms.

The force is recorded as a function of time. The displacement of the bottom grip is imposed at a constant speed of 0.001 mm s^{-1} leading to a strain rate of 6.6×10^{-5} s^{-1}.

The tomograph used for imaging is a VtomeX system manufactured by Phoenix X-Rays. It is described in more details in ref.[18] Local X-Ray tomography scans with a voxel size of 3 μm (the spot size was 2 μm during the acquisition) were first acquired with the sample mounted on the rig inside the tomograph in the unloaded stage. The purpose of the analysis is to obtain a good description of the microstructure and the internal defects before deformation. In this mode, the field of view of the detector in our system is about 4.5 mm in height and 5.7 mm in width only. To acquire an image of the entire sample, it was then necessary to perform 15 successive acquisitions, physically displacing the sample in a plane parallel to the detector between each acquisition to scan it in a different location (3 horizontal times 5 vertical displacements). These high-resolution reconstructions were used to detect the presence of inter-metallics and pores in the structure. The tomograph was operated with a 90 kV acceleration voltage using a tungsten transmission target with a 170 μA current. The spot size is about 2 μm in these conditions. The incident X-ray beam was not filtered. The reconstruction algorithm is a standard filtered back projection implemented in the software included in the commercial package of the tomograph.

It can be seen on the two gray level reconstructed slices shown in Figure 2a and b that the inter-metallics are clearly

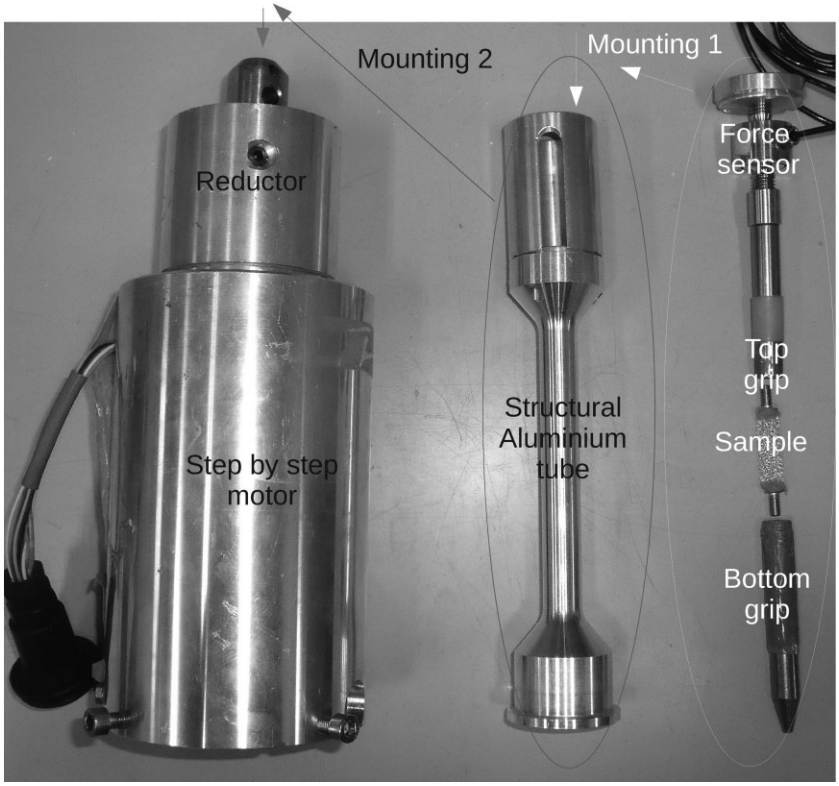

Fig. 1. Tensile device used for the in situ tensile test in the laboratory tomograph. The sample is first screwed in the top and bottom grip. The assembly is then mounted inside the structural aluminum tube (mounting 1). This is then mounted on the motor (mounting 2) and the entire set-up goes to the rotation stage of the tomograph.

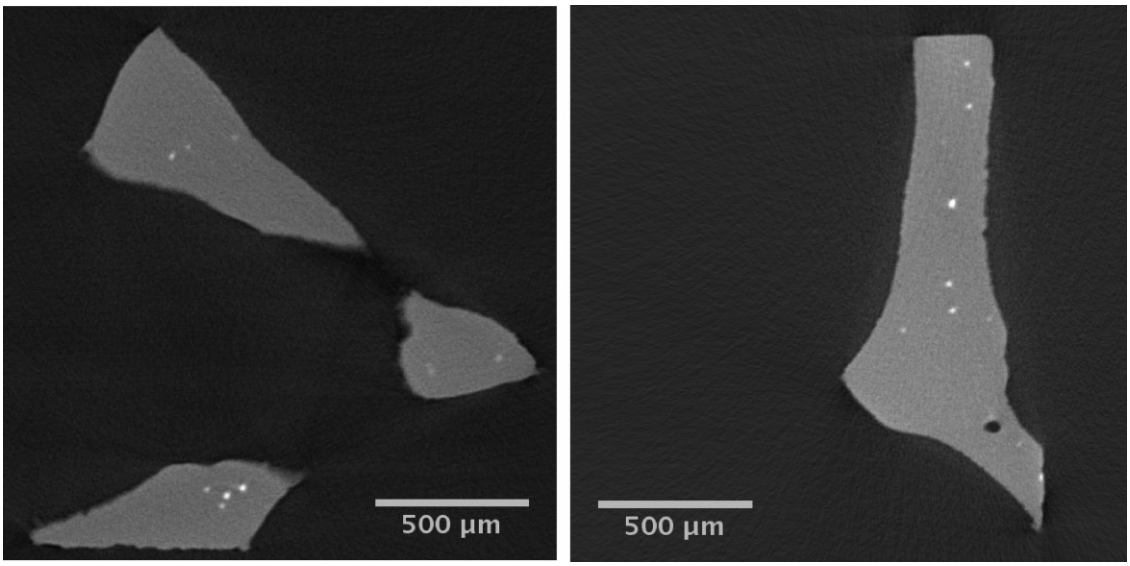

Fig. 2. Reconstructed slices at high resolution (local tomography condition) where the white inter-metallics and the black pores are detected.

detectable even though they are not fully resolved because 3 µm is not a good enough resolution for this purpose. It has been shown many times in the literature[19–21] that synchrotron images, with a resolution smaller than a micron are required for this rather. However, the quality of the images obtained at 3 µm with our laboratory tomograph, although not perfect, will be sufficient to detect the presence of the larger of these inter-metallics. It can also be seen in Figure 2 that pores are also present in the microstructure. To our knowledge, these pores are not frequently mentioned in the literature for ERG open cell foams. The fabrication process of these materials includes a casting step of the liquid alloy. This could lead to the formation of the observed pores. Another illustration of the type of results obtained is shown in Figure 3 where the total population of inter-metallics in one of the high resolution reconstructed scans is shown in 3D together with the outer surface of the struts, set transparent.

The sample was subsequently scanned in its initial state at low resolution (voxel size = 10 µm – with a spot size of about 2 µm – one scan is enough to view all sample) and then pulled and scanned again at 12 different deformation stages. The displacement of the tensile machine was stopped during acquisition and the acquisition time was 30 min. Figure 4 shows the tensile curve recorded during the experiment and a selection of renderings at three selected steps: initial state, just after the peak stress, and just before fracture. The strain at which these snapshots are extracted are indicated with arrows on the tensile curve. Struts were observed to start breaking just at the peak stress of the sample. The number of broken struts progressively increased while the size of the gaps created by the struts fractured earlier continued to grow (see Figure 5). In our experiment, we have observed that the location of the broken struts was quite localized, in the bottom half of the sample, where the final fracture takes place. We have carefully examined the microstructure away from this region and could not detect any other broken strut.

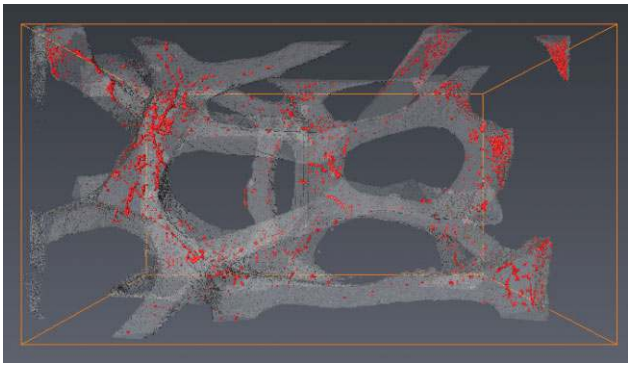

Fig. 3. 3D visualization of a full high resolution reconstructed scan showing the spatial distribution of the inter-metallics and the outer surface of the struts. The lateral size of the block is about 3 mm.

2. FE Simulation of the Local Stresses

The initial LXRCT image at low resolution (shown in Figure 5) was then used as an input to create a FEs mesh of the complex architecture of the full sample. This was achieved according to the procedure presented in ref.[9] The created mesh was composed of about 460 000 tetrahedrons. It was used to perform a calculation using the abaqus™ commercial code. In terms of boundary conditions, the nodes at the top of the model were displaced of a fixed value along the tensile direction while the nodes at the bottom were maintained in their initial position along this direction only and set free to move in the two other directions. For the sake of simplicity, the calculation was performed in the elastic regime (Young's modulus and Poisson's ratio values of the solid aluminum were chosen to be 70 GPa and 0.33, respectively). This preliminary calculation was only aimed at evaluating the

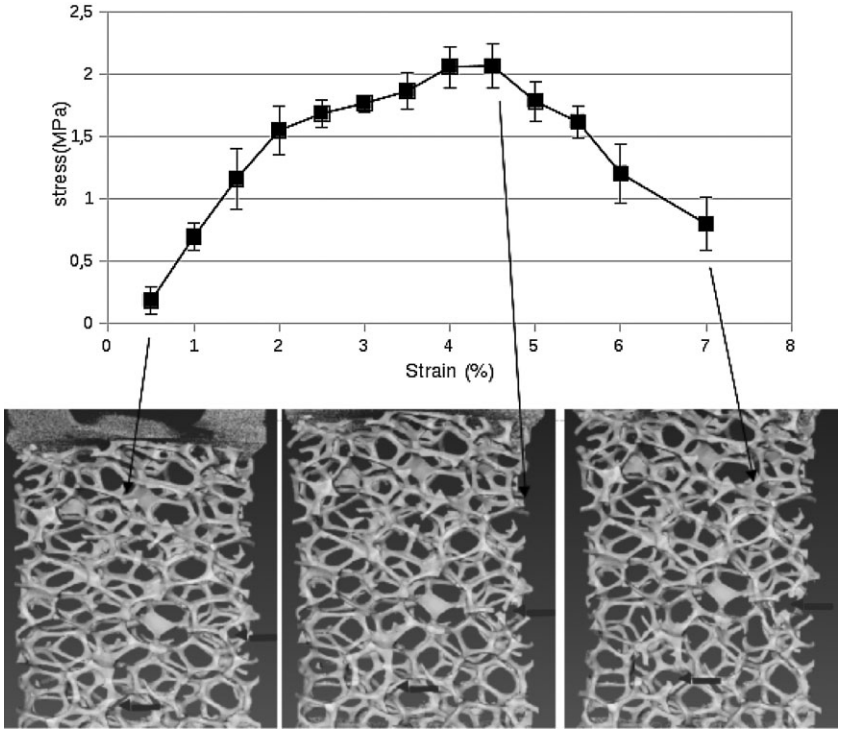

Fig. 4. Low resolution reconstruction of the sample during the in situ tensile test at tensile strains equal to 0, 5, and 7%. The width of the specimen is 10 mm.

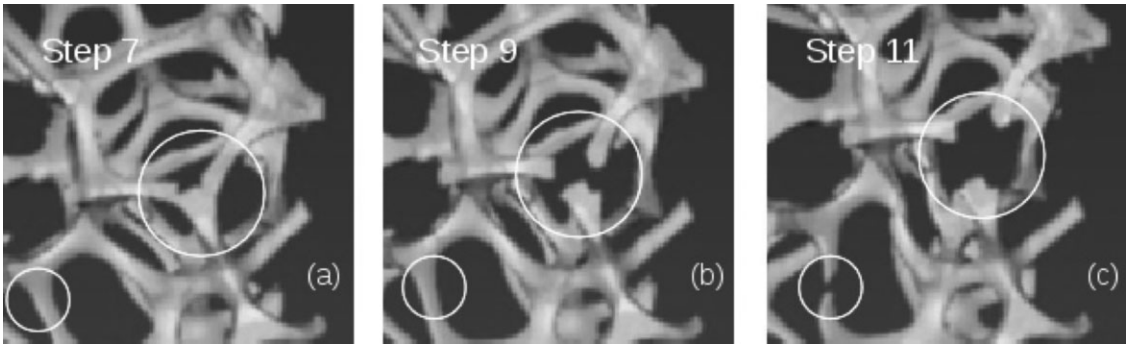

Fig. 5. Detail of the fracture process showing the growth of a gap induced by the fracture of a strut (here the fracture of two struts at the same node).

local values of the stresses in every location of the sample. A more complex calculation including plasticity would be required to simulate the tensile curve but this is not attempted in the present work. Figure 6a shows a contour plot of the local value of the von Mises stress calculated using the model. The regions where the sample is highly stressed can be visualized by a lighter value of the color in this rendering. Figure 6b shows as a comparison, a detailed LXRCT view of the region where the sample has broken, extracted in step 11, just before fracture. The black circles highlight locations where highly stressed struts have broken. This type of observation was anticipated because the highly stressed struts are more likely to break. The white circles however, show regions where the fracture has occurred in a strut for which the prediction of the local stress is not very high. This seems to indicate that the material could be locally weaker in the regions, leading to a premature fracture of the struts.

Figure 7a and b shows higher magnification images of the two regions where the fracture was detected in moderately loaded struts. The figures at the top show the von Mises contour plot in the model and the bottom figures show the internal structure in these exact locations as images using the high resolution local tomography in the initial state. The bottom figures also include a low resolution 3D rendering obtained from the scan in the deformed state 11 to show how the strut broke. In the high resolution local tomography images, we have highlighted the presence of the inter-metallics in red. These are visible because the interface between air and the solid aluminum has been set transparent in the rendering. Pores can also be observed in black in these

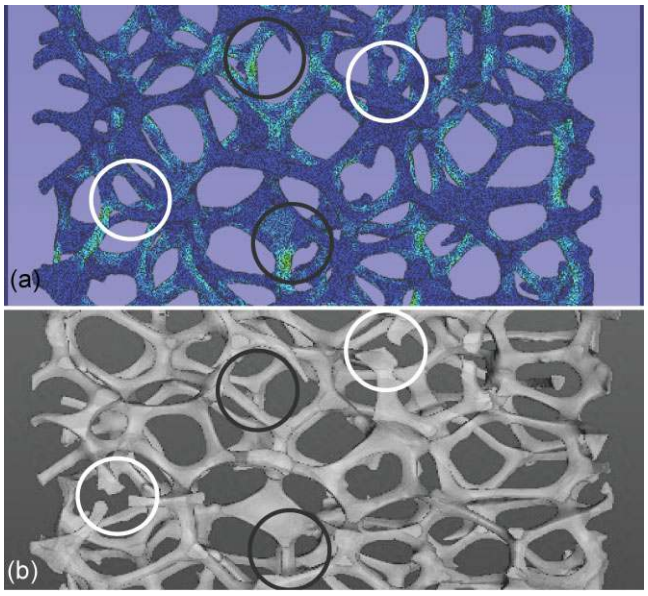

Fig. 6. Contour plot of the von Mises stress after a simulated tensile elastic strain to highlight regions where the stress is high in the model (a). Experimental observation of the broken sample (b).

figures. It becomes clear from these results that the fracture of the moderately loaded struts can be related to the presence of pores or inter-metallics. Using equivalent images, not shown in the present paper, we have noticed that in the case of the fracture of the two highly loaded struts shown in Figure 6 (highlighted by black circles), the amount of inter-metallics is much smaller.

3. Conclusions

In this paper, we have presented an experimental investigation of the microstructure of an ERG foam and its evolution during an in situ tensile test. Prior to deformation, the internal structure of the solid material constituting the foam was studied by high resolution local tomography leading to a detailed information of the location of intermetallics in the sample. We have evidenced the presence of large pores in the aluminum. The fracture process of the material during tension was then captured using low resolution scans during a high number of deformation steps of the foam. Fracture of the struts and opening of the so created gaps was clearly visible. The low resolution scan in the initial state was also used as input for an image-based FE calculation leading to the detection of regions where the stresses are high in the material. In the fracture zone, some of the broken struts were highly loaded while some others where much less loaded. The local tomography high resolution images in the initial state revealed the presence of large defects (pores and inter-metallics) in the moderately loaded broken struts, evidencing that the local microstructure plays a key role in the initiation of fracture. Finally, it can be anticipated that this kind of method could help very much to optimize (and perhaps predict) the rupture properties of these materials

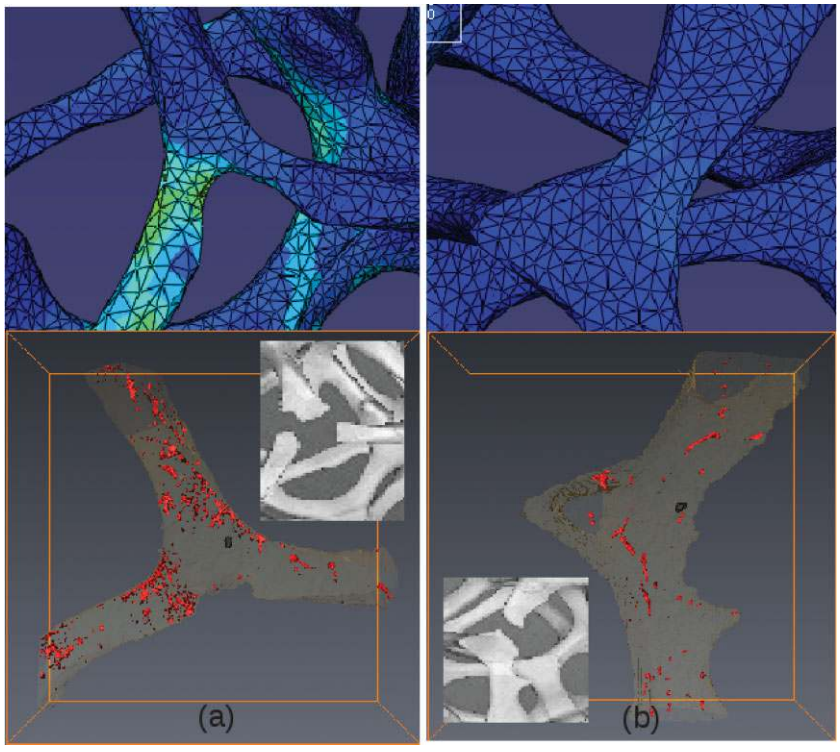

Fig. 7. Comparison between the FE calculation of the local stress and the internal distribution of inter-metallics and pores in moderately loaded struts.

as a predictive tool (without needing to tensile test) using the FE model for local stress and knowing the local concentrations of defects (and their effect on the fracture strain).

Received: January 4, 2013
Final Version: February 27, 2013
Published online: April 30, 2013

[1] L. J. Gibson, *Annu. Rev. Mater. Sci.* **2000**, *30*, 191.
[2] H. Bart-Smith, A. F. Bastawros, D. R. Mumm, A. G. Evans, D. J. Sypeck, H. N. G. Wadley, *Acta Mater.* **1998**, *46*, 3582.
[3] G. Gioux, T. M. McCormack, L. J. Gibson, *Int. J. Mech. Sci.* **2000**, *42*, 1097.
[4] B. K. Bay, T. S. Smith, D. P. Fyhrie, M. Saad, *Exp. Mech.* **1999**, *39*, 218.
[5] L. Helfen, T. Baumbach, H. Stanzick, J. Banhart, A. Elmoutaouakkil, P. Cloetens, K. Schladitz, *Adv. Eng. Mater.* **2002**, *4*, 808.
[6] O. B. Olurin, M. Arnold, C. Körner, R. F. Singer, *Mat. Sci. Eng A* **2002**, *328*, 2002.
[7] O. Caty, E. Maire, T. Douillard, P. Bertino, R. Dejaeger, R. Bouchet, *Mater. Lett.* **2009**, *63*, 1131.
[8] S. A. McDonald, G. Dedreuil-Monet, Y. T. Yao, A. Alderson, P. J. Withers, *Phys. Status Solidi B* **2011**, 24845-51.10.
[9] S. Youssef, E. maire, R. Gaertner, *Acta Mater.* **2005**, *53*, 719.
[10] O. Caty, E. Maire, S. Youssef, R. Bouchet, *Acta Mater.* **2008**, *56*, 5524.
[11] N. Michailidis, F. Stergioudi, H. Omar, D. Tsipas, *Comput. Mater. Sci.* **2010**, *48*, 282.
[12] H. Toda, T. Ohgaki, K. Uesugi, M. Kobayashi, N. Kuroda, T. Kobayashi, M. Niinomi, T. Akahori, K. Makii, Y. Aruga, *Metall. Mater. Trans. A.* **2006**, *37A*, 1211.
[13] N. Michailidis, F. Stergioudi, H. Omar, D. Papadopoulos, D. N. Tsipas, *Colloids Surf. A Physicochem. Eng. Aspects* **2011**, *382*, 124.
[14] A. E. Markaki, T. W. Clyne, *Acta Mater.* **2001**, *49*, 1677.
[15] E. Amsterdam, J. Th. M. De Hosson, P. R. Onck, *Acta Mater.* **2006**, *54*, 4465.
[16] E. Amsterdam, J. H. B. de Vries, T. Th. M. De Hosson, P. R. Onck, *Acta Mater.* **2008**, *56*, 609.
[17] E. Amsterdam, P. R. Onck, J. Th. M. De Hosson, *J. Mater. Sci.* **2005**, *40*, 5813.
[18] J.-Y. Buffiere, E. Maire, J. Adrien, J.-P. Masse, E. Boller, *Exp. Mech.* **2010**, *50*, 289.
[19] E. Maire, J. C. Grenier, D. Daniel, A. Baldacci, H. Klöcker, A. Bigot, *Scr. Mater.* **2006**, *55*, 123.
[20] G. Requena, P. Cloetens, W. Altendorfer, C. Poletti, D. Tolnai, F. Warchomicka, H. P. Degischer, *Scr. Mater.* **2009**, *61*, 760.
[21] Z. Asghar, G. Requena, E. Boller, *Acta Mater.* **2011**, *59*, 6420.